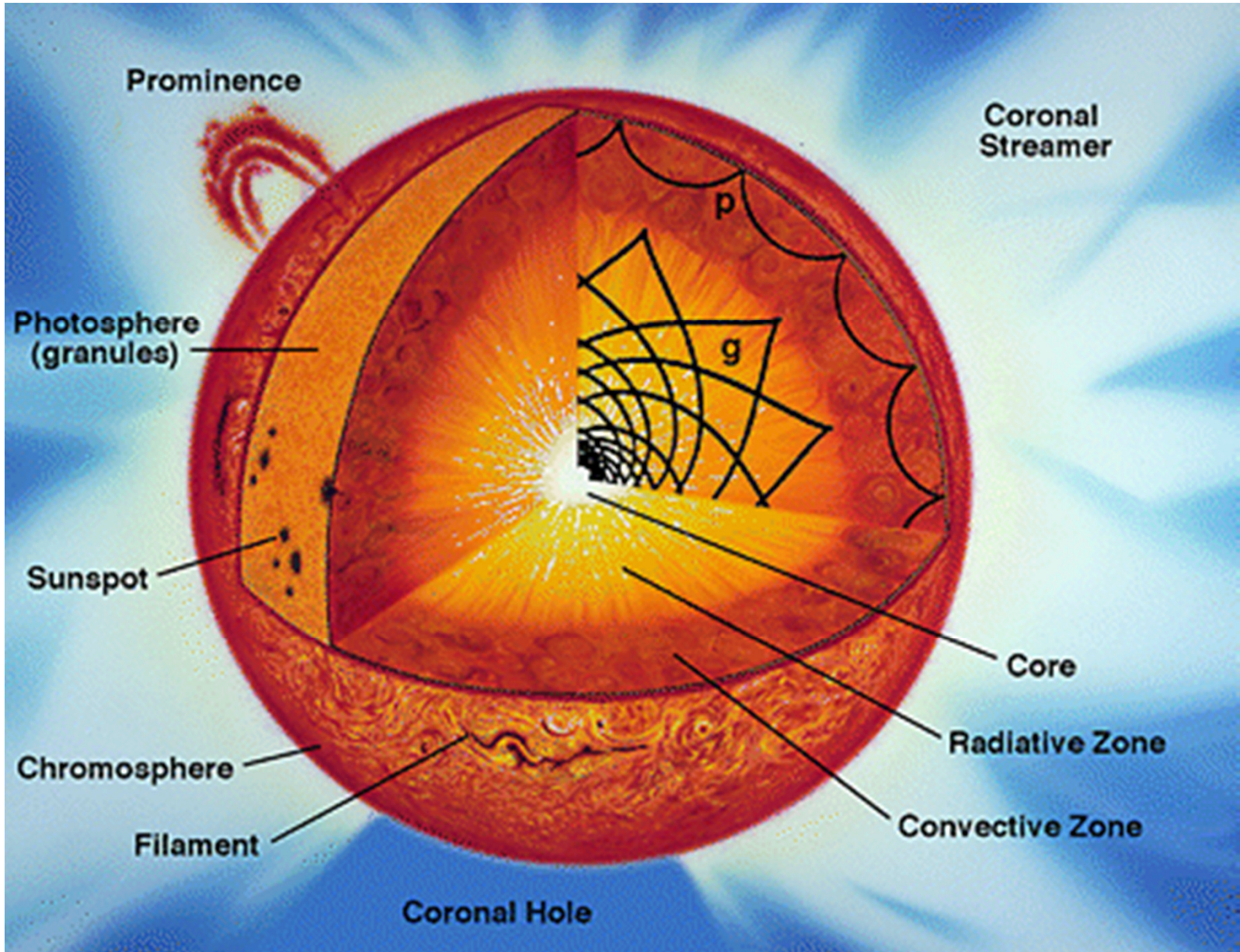


12. Solar Convection

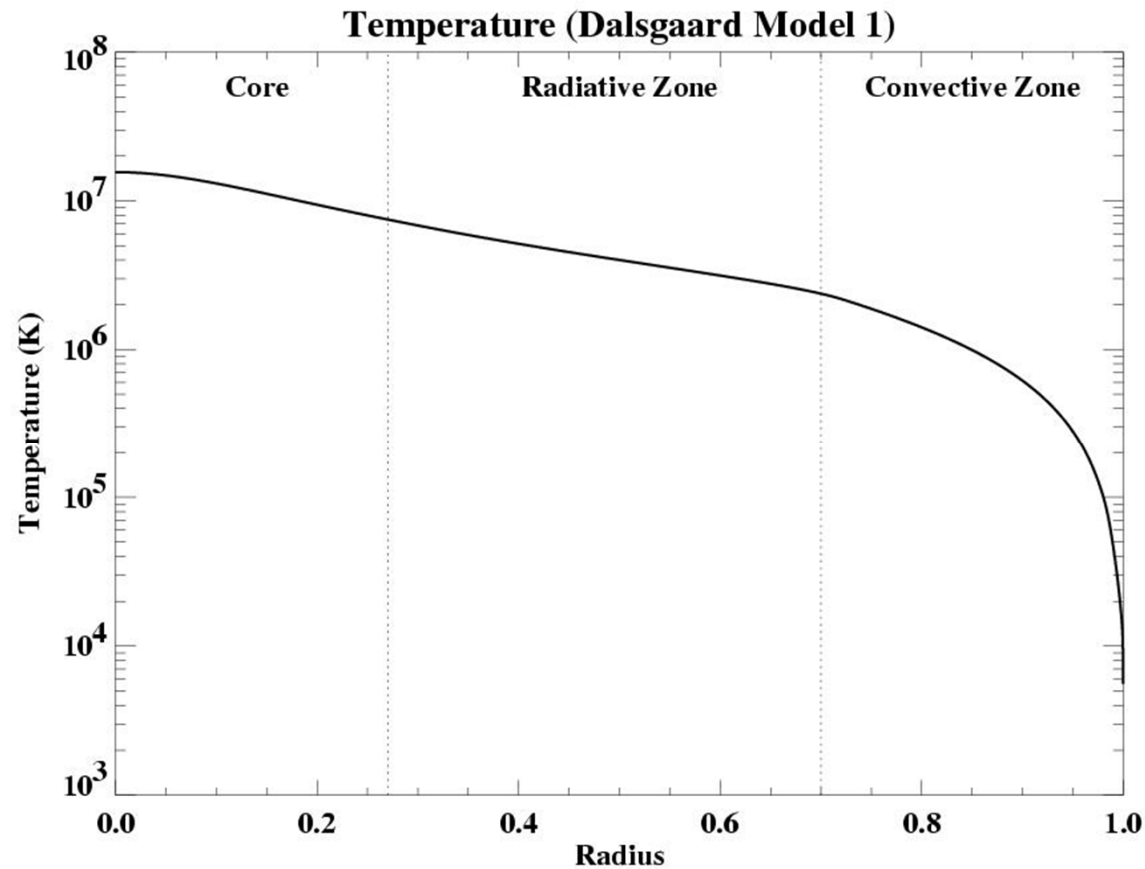
Solar Convection

- Convection Zone
- Convective Instability
- Convective Energy Transport
- Mixing-Length Theory
- Convective overshoot
- Observation of Solar Convection
 - Granulation
 - Supergranulation
 - Search for giant cells
- Numerical Simulations of Solar Convection

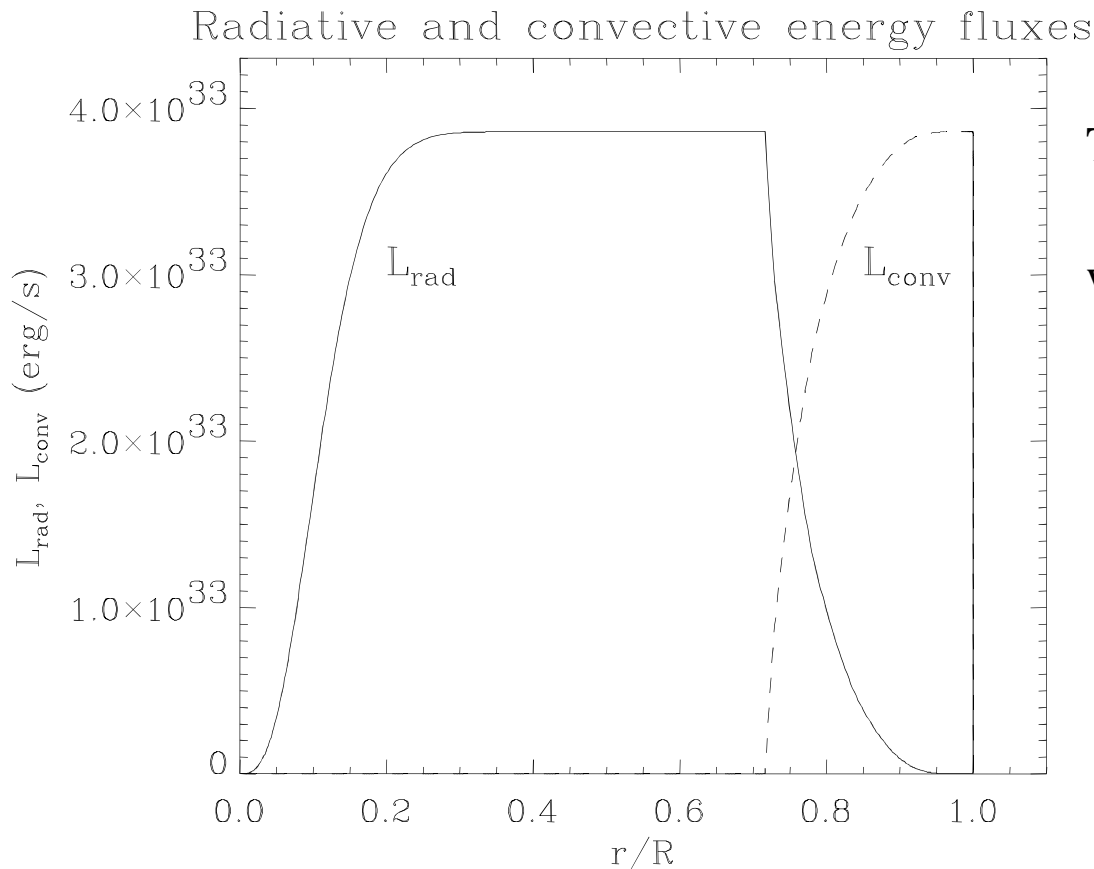


Origin of the solar convection zone

Convection occurs because the temperature gradient becomes steeper than the ‘adiabatic temperature gradient’. The temperature gradient becomes steeper in the outer layers of the Sun because the temperature there is lower than in the temperature in the radiative core, and thus it requires a stronger dT/dr to keep the radiative energy flux, $\propto T^3(dT/dr)$. When the solar plasma becomes convectively unstable most of the solar energy is transported by convection.



Radiative and convective energy fluxes



The total energy flux is

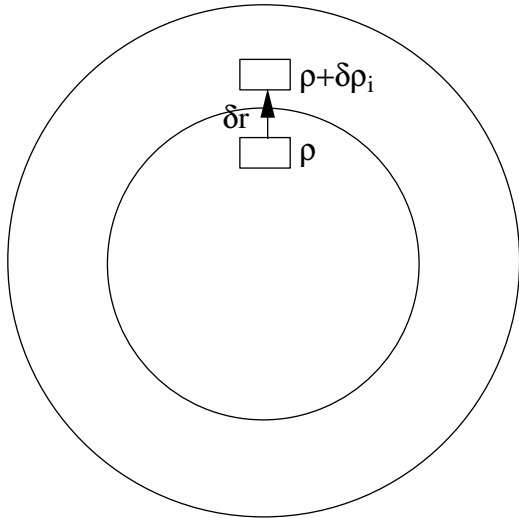
$$L_{\text{rad}} + L_{\text{conv}} = L_{\odot},$$

where

$$\begin{aligned} F_{\text{rad}} &\equiv \frac{L_R}{4\pi r^2} = \\ &= -\frac{16\sigma T^3}{3\kappa\rho} \frac{dT}{dr} \equiv \frac{16\sigma T^4}{3\kappa\rho H_p} \nabla \end{aligned}$$

$$\nabla \equiv \frac{\partial \log T}{\partial \log P}.$$

Convective instability



Consider a displacement, δr , of a small fluid element along the radius. If the density inside the displaced element, $\rho + \delta\rho_i$ is smaller the density of surrounding plasma, $\rho + \delta\rho$, then the element will continue moving up under the buoyancy force. Therefore, the condition of the convective instability is:

$$\Delta\rho \equiv \delta\rho_i - \delta\rho < 0.$$

Physical conditions inside the element obey the adiabatic law because the characteristic time for heat exchange is much longer than the dynamic time. Then,

$$\delta\rho_i = \left(\frac{d\rho}{dr} \right)_{\text{ad}} \delta r = \frac{\rho}{\gamma P} \left(\frac{dP}{dr} \right) \delta r, \quad (\text{use the adiabatic law } P / \rho^\gamma = \text{const})$$

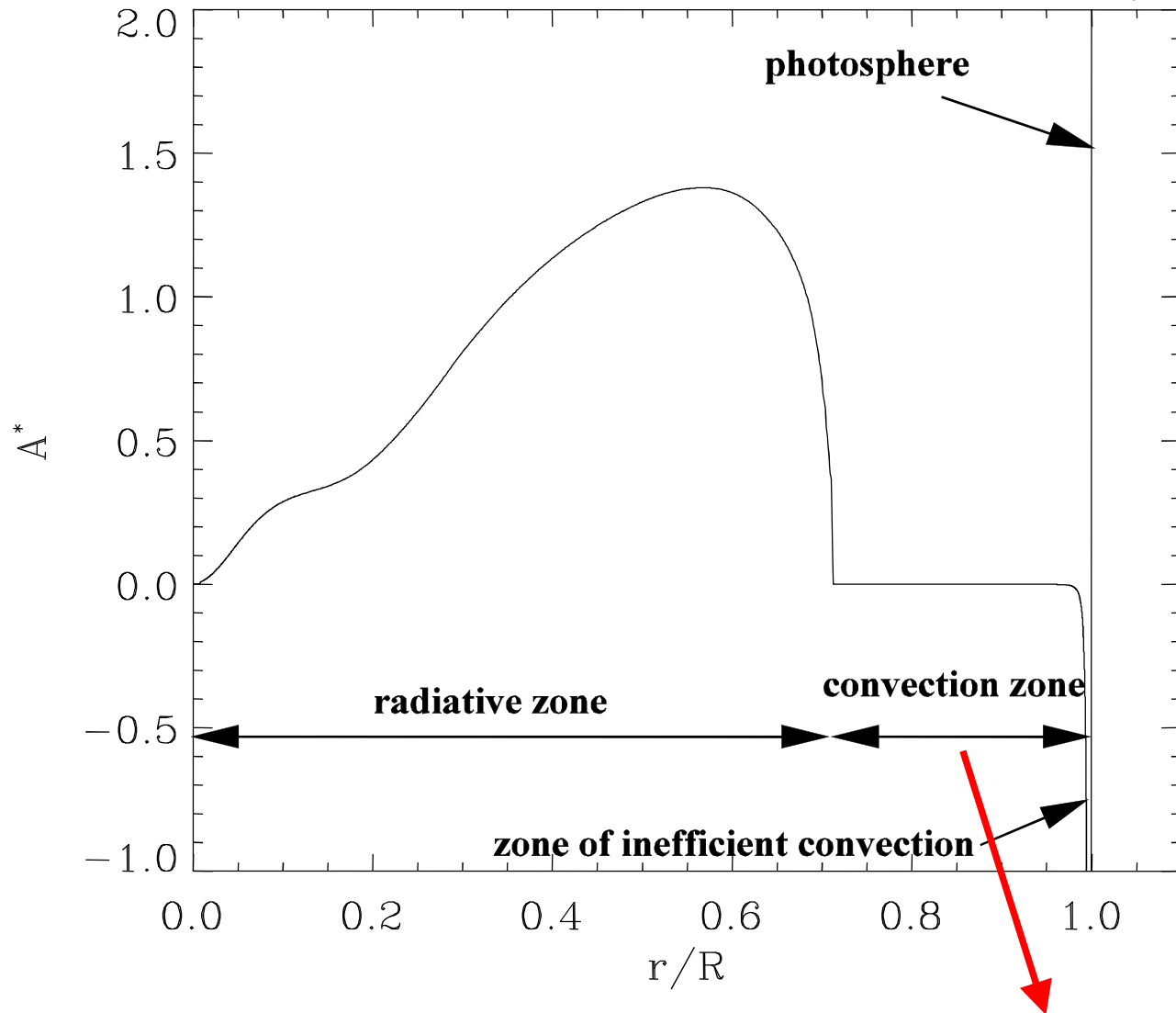
where γ is the adiabatic exponent. The density variation in the surrounding plasma

$$\text{is: } \delta\rho = \frac{d\rho}{dr} \delta r. \quad \text{Then, } \Delta\rho \equiv \delta\rho_i - \delta\rho = \frac{d\rho}{dr} \delta r - \frac{\rho}{\gamma P} \left(\frac{dP}{dr} \right) \delta r < 0.$$

$$\text{Finally, the instability condition is: } A^* \equiv \frac{1}{\gamma} \frac{d \log P}{d \log r} - \frac{d \log \rho}{d \log r} < 0.$$

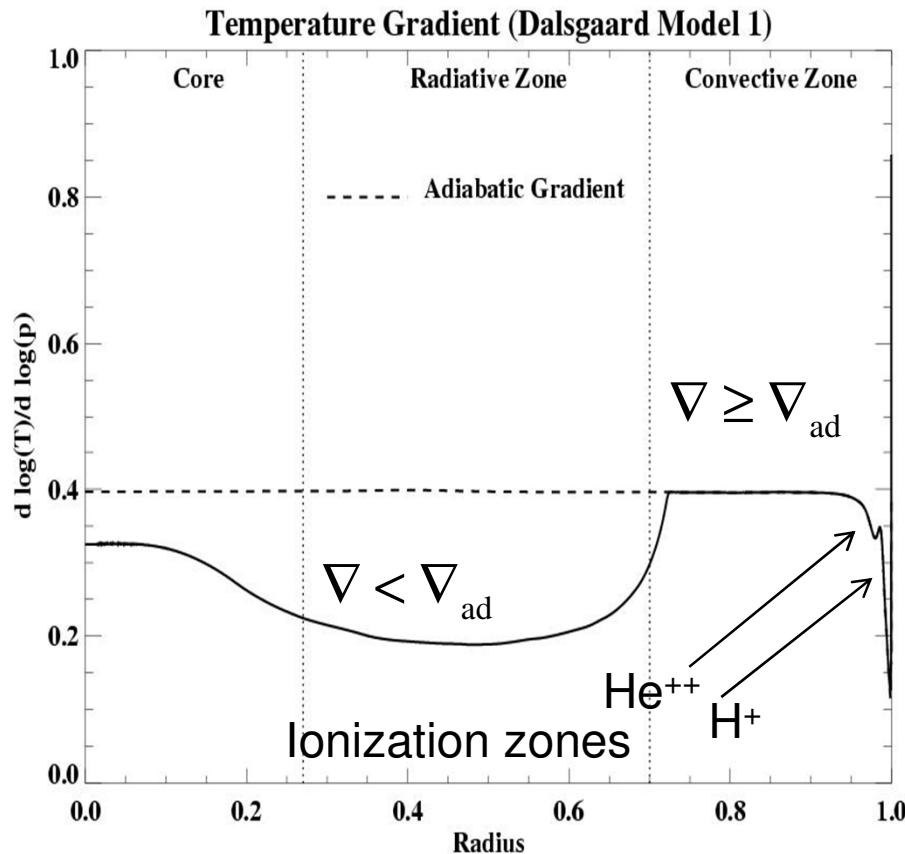
Parameter A^* is called the Ledoux parameter of convective stability.

Parameter of convective stability



$$A^* \equiv \frac{1}{\gamma} \frac{d \log P}{d \log r} - \frac{d \log \rho}{d \log r} < 0, \text{ or equivalently } N^2 < 0$$

Convective instability in terms of temperature gradients



By using the equation of state, $\rho = \frac{P\mu}{\mathcal{R}T}$ and assuming $\mu = \text{const}$, the condition of instability can be expressed in terms of temperature gradients:

$$\left(\frac{dT}{dr} \right)_{ad} - \frac{dT}{dr} > 0,$$

Using the equation of hydrostatic equilibrium: $dP/dr = -g\rho$, we write:

$$\nabla_{ad} - \nabla < 0, \text{ or } \nabla > \nabla_{ad}$$

$\nabla_{ad} \equiv \left(\frac{d \log T}{d \log P} \right)_{ad}$ is the 'adiabatic gradient',

$\nabla \equiv \left(\frac{d \log T}{d \log P} \right)$ is the 'local (ambient) gradient'.

For an ideal gas $\nabla_{ad} \simeq \frac{\gamma-1}{\gamma}$, thus the instability occurs when $\nabla > \frac{\gamma-1}{\gamma}$.

In fully ionized gas $\gamma = 5/3$; thus, $\nabla = (\gamma-1)/\gamma = 0.4$ in the ionization zones $\gamma < 5/3$, such zones are more unstable.

Effect of molecular weight gradients on convective instability

Consider effects of variations of the molecular weight μ .

Equation of state: $\rho = \frac{P\mu}{\mathcal{R}T}$.

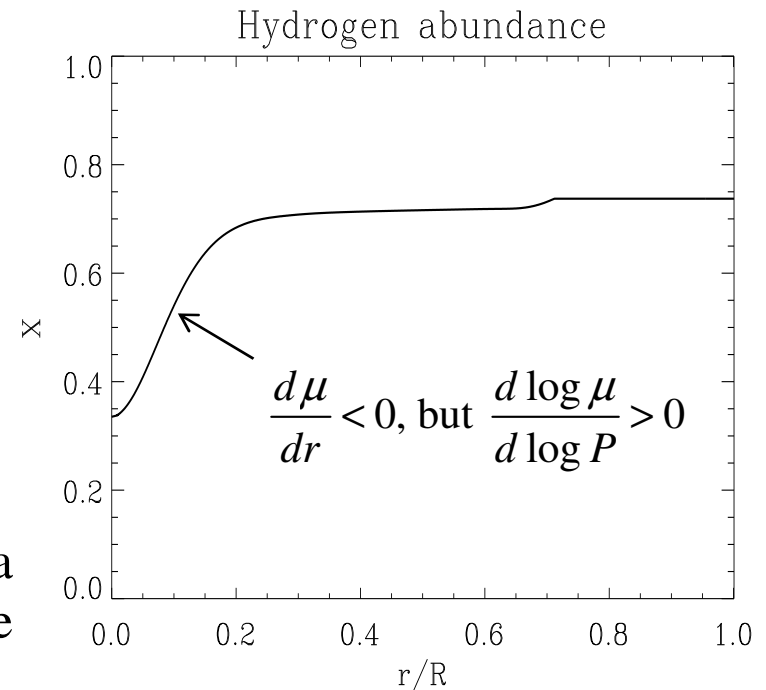
Changes in μ can arise from ionization and nuclear reactions. For variable μ the condition for convective instability is:

$$\frac{dT}{dr} < \left(\frac{dT}{dr} \right)_{\text{ad}} + \frac{T}{\mu} \frac{d\mu}{dr} - \frac{T}{\mu} \left(\frac{d\mu}{dr} \right)_{\text{ad}}.$$

Consider this condition in the solar core where plasma is fully ionized, and thus ionization does not change under adiabatic conditions, that is, $(d\mu/dr)_{\text{ad}} = 0$. Because of nuclear reactions, $d\mu/dr < 0$. Therefore, this gradient is stabilizing.

The instability condition is $\nabla > \nabla_{\text{ad}} + \nabla_{\mu}$,

where $\nabla_{\mu} = \frac{d \log \mu}{d \log P}$.

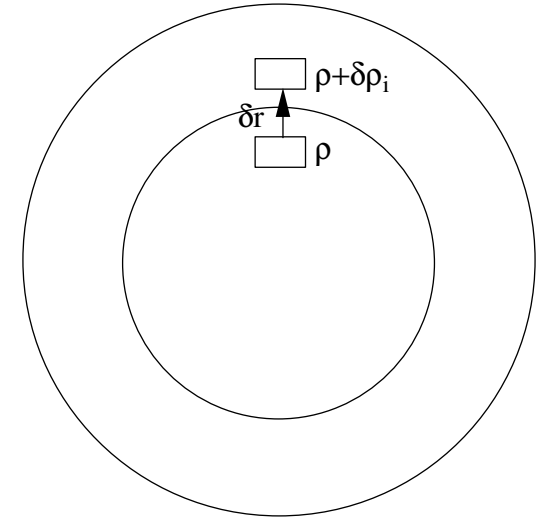


Because of nuclear reactions the solar core has more helium than the rest of the Sun. Thus, the molecular weight decreases with the radius.

Convective Energy Transport: Mixing-Length Theory

Consider the momentum equation of a fluid element:

$$\begin{aligned} \rho \frac{d^2 \delta r}{dt^2} &= -g \Delta \rho = -g \left[\left(\frac{d\rho}{dr} \right)_{\text{ad}} - \frac{d\rho}{dr} \right] \delta r = \\ &= -g \rho \left[\left(\frac{d \log \rho}{dr} \right)_{\text{ad}} - \frac{d \log \rho}{dr} \right] \delta r = \\ &= -g \rho \left[\left(\frac{d \log T}{d \log P} \right)_{\text{ad}} - \frac{d \log T}{d \log P} \right] \frac{1}{H_p}, \end{aligned}$$



where $\frac{1}{H_p} = -\frac{d \log P}{dr}$ is the pressure scale height.

Finally, $\frac{d^2 \delta r}{dt^2} = -\frac{g}{H_p} (\nabla_{\text{ad}} - \nabla) \delta r = -N^2 \delta r,$

where $N^2 = \frac{g}{H_p} (\nabla_{\text{ad}} - \nabla)$ is the Brunt-Väisälä frequency; $N^2 = \frac{g}{r} A^*$ in term of the

Ledoux parameter of convective stability; $A^* = \frac{1}{\gamma} \frac{d \log P}{d \log r} - \frac{d \log \rho}{d \log r}$

If $N^2 < 0$ then the medium is convectively unstable.

If $N^2 > 0$ then it is convectively stable: $\delta r \propto \sin(Nt)$; the fluid elements oscillate with frequency N . These oscillations are called internal gravity waves - g-modes.

Convective Energy Flux

Multiply the momentum equation by $2\frac{d\delta r}{dt}$ and integrate over t :

$$\left(\frac{d\delta r}{dt}\right)^2 = \frac{g}{H_p}(\nabla - \nabla_{\text{ad}})\delta r^2.$$

The mixing-length theory assumes that the convective elements travel without destruction a distance l - 'mixing length':

$$\overline{\delta r} = l/2.$$

Then, the characteristic velocity, v , of these elements can be estimated as:

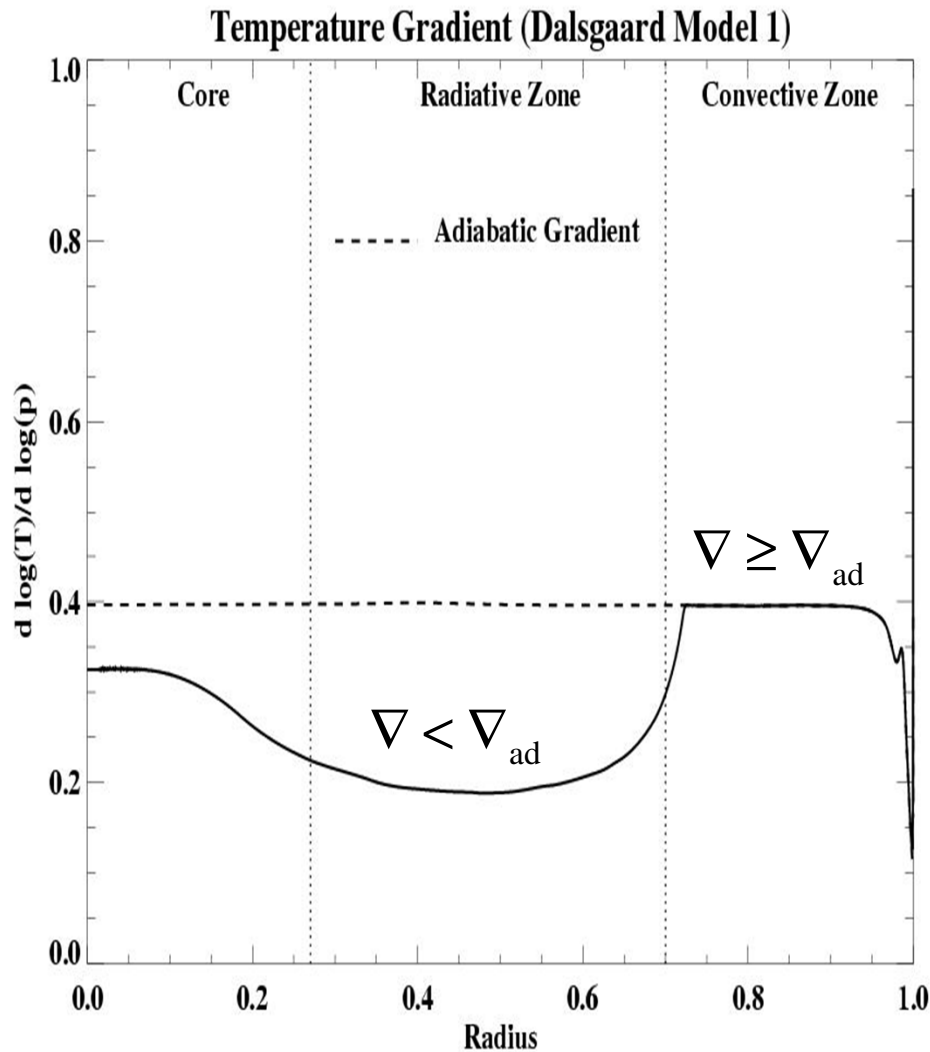
$$v^2 = \frac{g}{4H_p}(\nabla - \nabla_{\text{ad}})l^2.$$

Then, the convective energy flux is:

$$F_c = \rho v^3 = \rho \left(\frac{g}{4H_p}(\nabla - \nabla_{\text{ad}})l^2 \right)^{3/2}.$$

In the convection zone, ∇ is slightly greater than ∇_{ad} . This is sufficient to carry the energy flux; the convective velocity is small in this regime, which is called 'efficient convection'.

Mixing-length parameter



$$F_c = \rho v^3 = \rho \left(\frac{g}{4H_p} (\nabla - \nabla_{\text{ad}}) l^2 \right)^{3/2}.$$

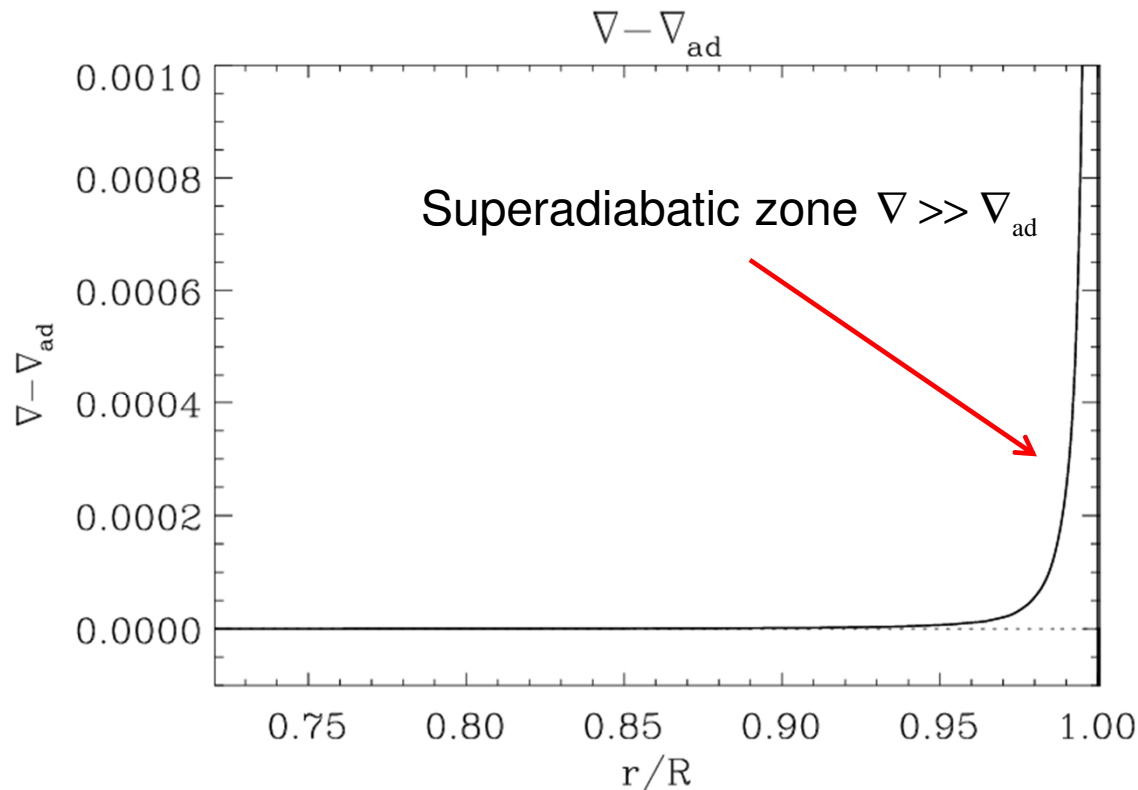
The mixing length is usually defined in terms of the pressure scale height:

$$l = \alpha H_p,$$

where α is called ‘**the mixing length parameter**’. $H_p = -\left(\frac{d \log P}{dr}\right)^{-1}$ is the pressure scale height.

In the convection zone, ∇ is slightly greater than ∇_{ad} . This is sufficient to carry the energy flux; the convective velocity is small in this regime, which is called ‘efficient convection’.

Superadiabatic gradient



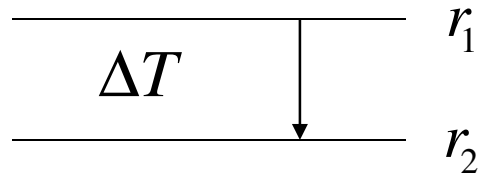
$$F_c = \rho v^3 = \rho \left(\frac{g}{4H_p} (\nabla - \nabla_{\text{ad}}) l^2 \right)^{3/2}$$

Near the solar surface where the density, ρ , is small much higher, near sonic velocity, is required to transport the solar energy. In this case $\nabla \gg \nabla_{\text{ad}}$. This near surface zone is called a 'superadiabatic zone'.

Convective overshoot

Convective overshoot is penetration of convective elements into convectively stable layers. Evidence for convective overshoot at the base of the convection zone is the observed deficit of Li and Be. These elements are burned in nuclear reactions in the upper radiative zone where they are transported by overshoot.

The overshoot is described by a non-local mixing length theory.



Consider plasma elements starting at level r_1 . At level r_2 the mean temperature excess, ΔT , and velocity, v , of these elements is given by

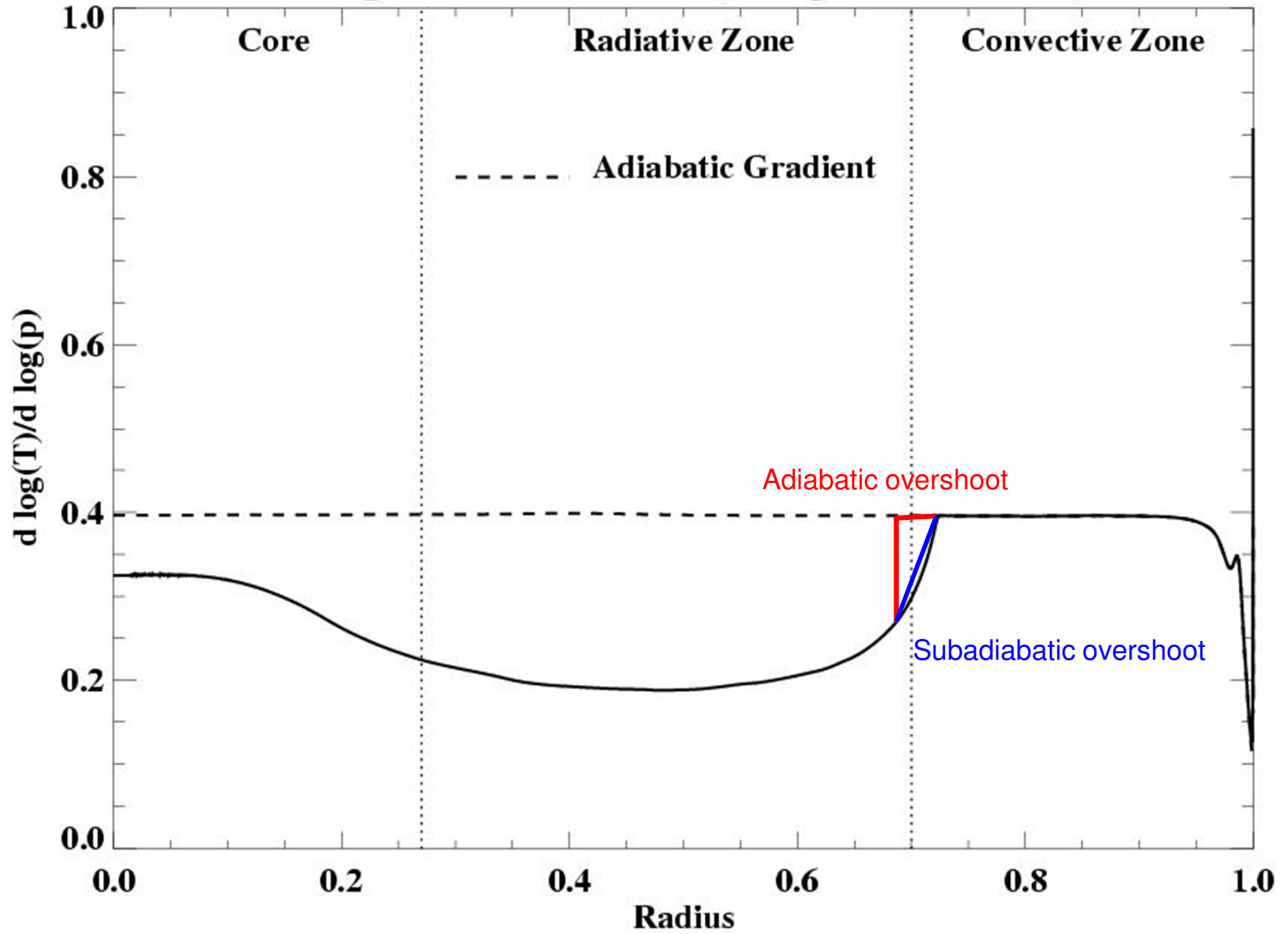
$$\Delta T(r_2, r_1) = -\int_{r_1}^{r_2} \left[\frac{dT}{dr} - \left(\frac{dT}{dr} \right)_{\text{ad}} \right] dr,$$

and the balance of the kinetic energy and buoyancy work:

$$\frac{1}{2} v^2(r_2, r_1) = \int_{r_1}^{r_2} \frac{g}{T} \Delta T(r, r_1) dr.$$

The mixing-length theory assumes that for rising elements $r_2 = r_1 + l$, and for sinking elements $r_2 = r_1 - l$.

Temperature Gradient (Dalsgaard Model 1)



Overshoot model of Stix and Skaley (1991) may explain the sound-speed bump (in $\delta c / c$) at the base of the convection zone found by helioseismology

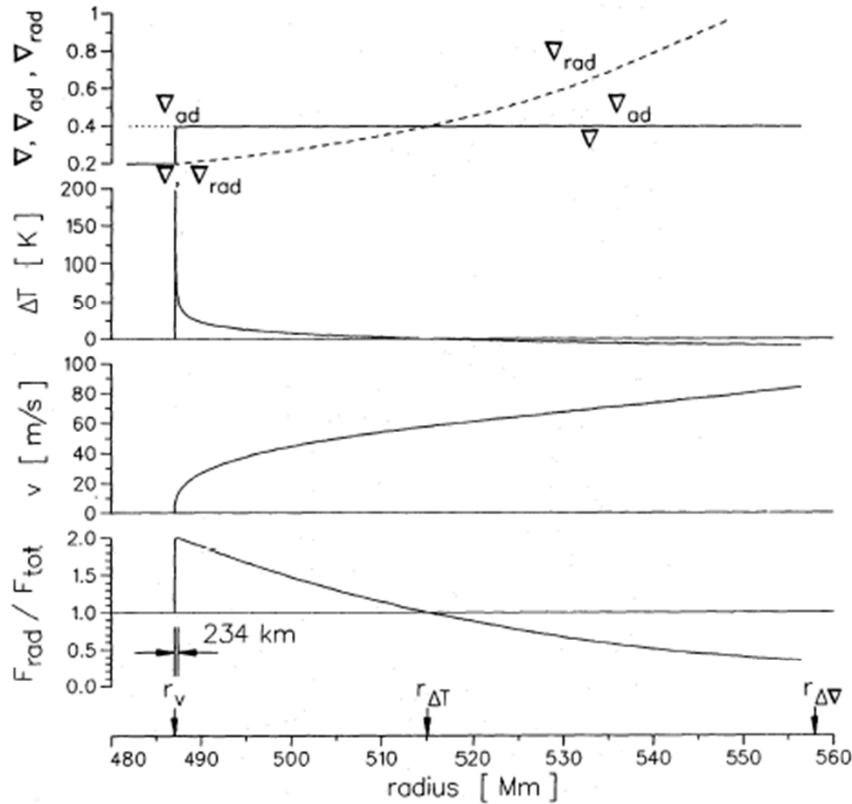


Fig. 1. Overshoot layer of model 3. Real, adiabatic and radiative temperature gradients ∇ , ∇_{ad} , and ∇_{rad} ; temperature excess ΔT , of sinking parcels; absolute value of the mean convective velocity v as calculated from eq. (5), normalized to the value arising from the local theory at r_{fit} and the quotient, F_{rad}/F_{tot} , of the radiative and total energy fluxes

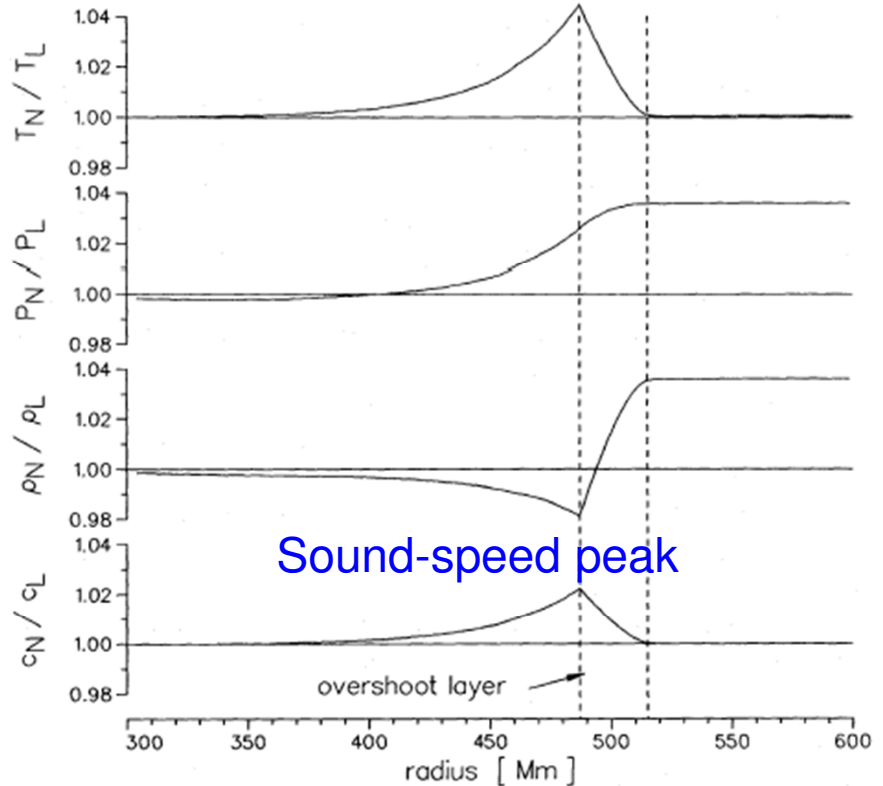
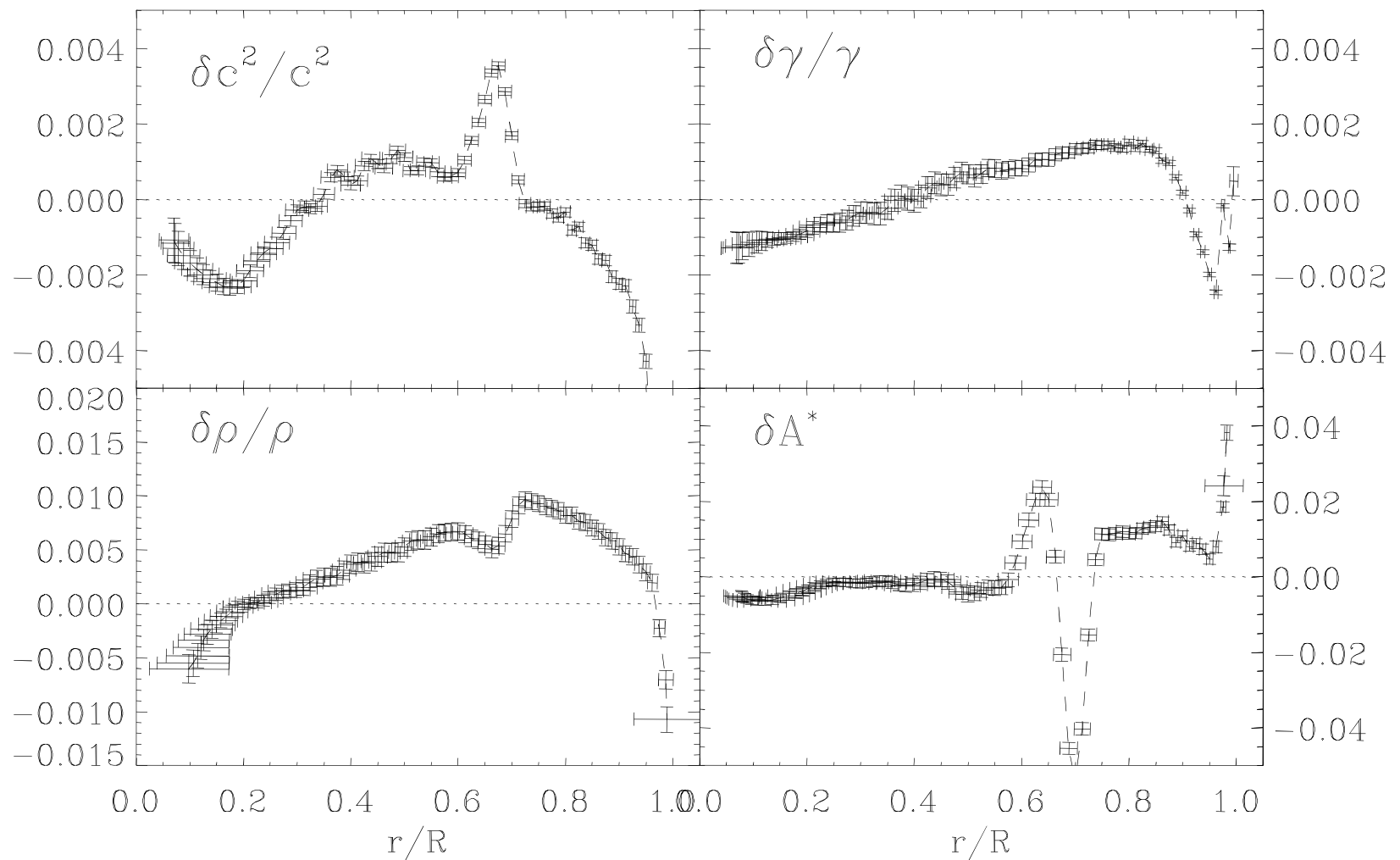


Fig. 6. Ratio of the variables: temperature T , pressure P , density ρ , and speed of sound c of model 3, with non-local MLT (N), and model 1, with local MLT (L)

Inversion results for the observed solar frequencies



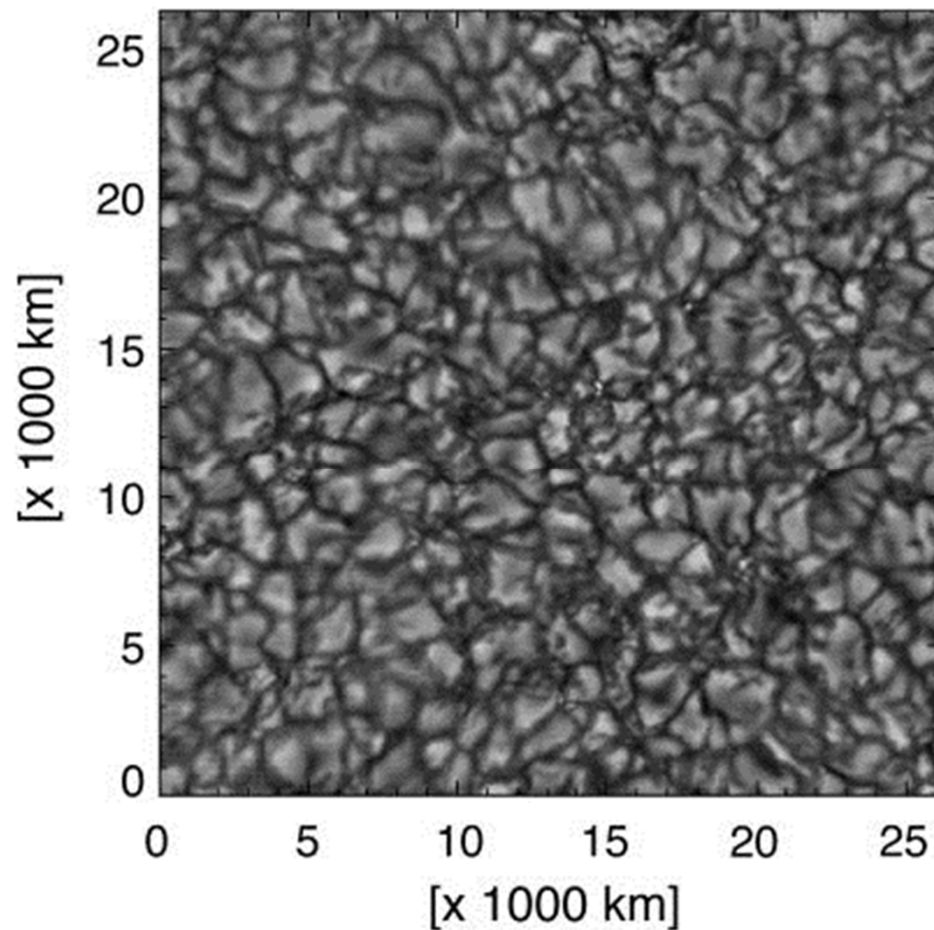
Observation of Solar Convection

Convection cells:

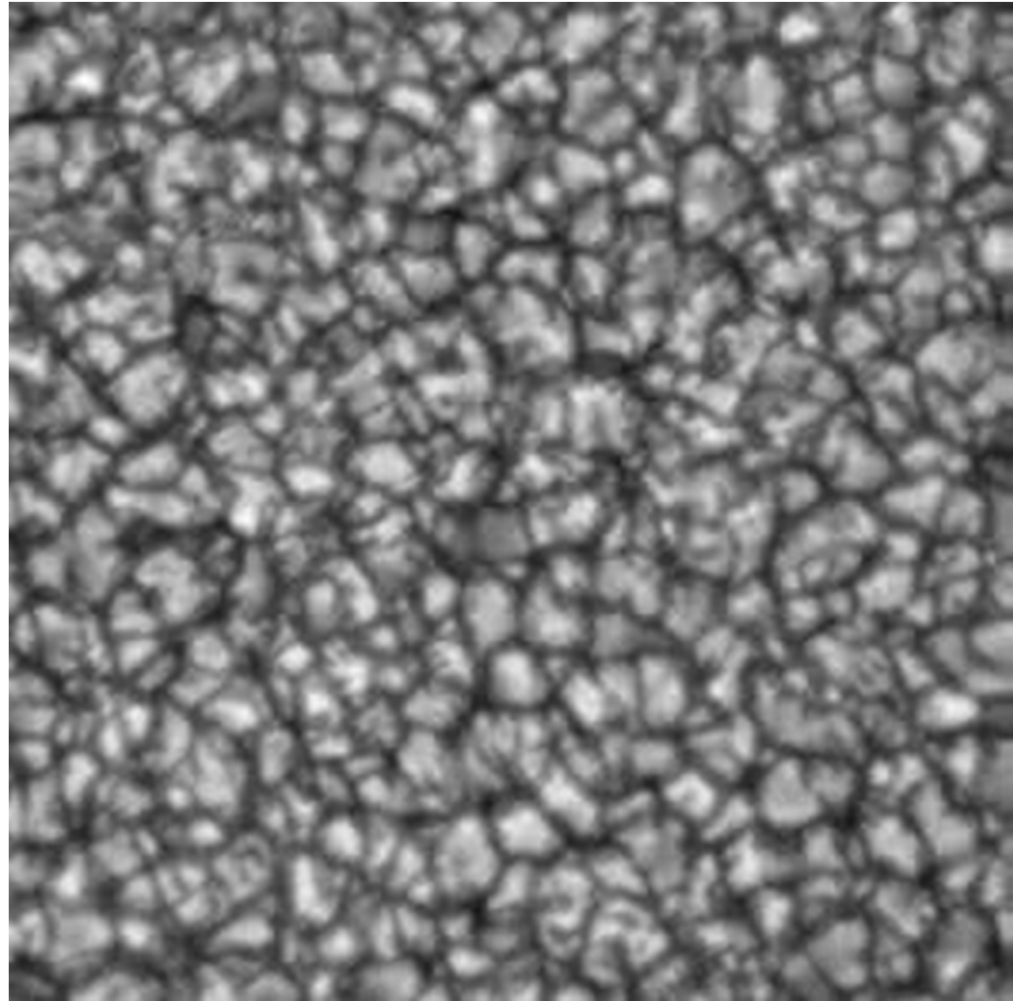
- Granulation (size $\sim 10^3$ km, lifetime ~ 10 min, velocity ~ 1 km/s).
- Mesogranulation (size $\sim 10^4$ km, lifetime ~ 1 hour, velocity ~ 1 km/s).
- Supergranulation (size $\sim 3 \times 10^4$ km, lifetime ~ 1 day, velocity ~ 0.5 km/s).
- Giant cells (?) (size $> 10^5$ km, lifetime > 1 months, velocity < 0.1 km/s).

Granulation

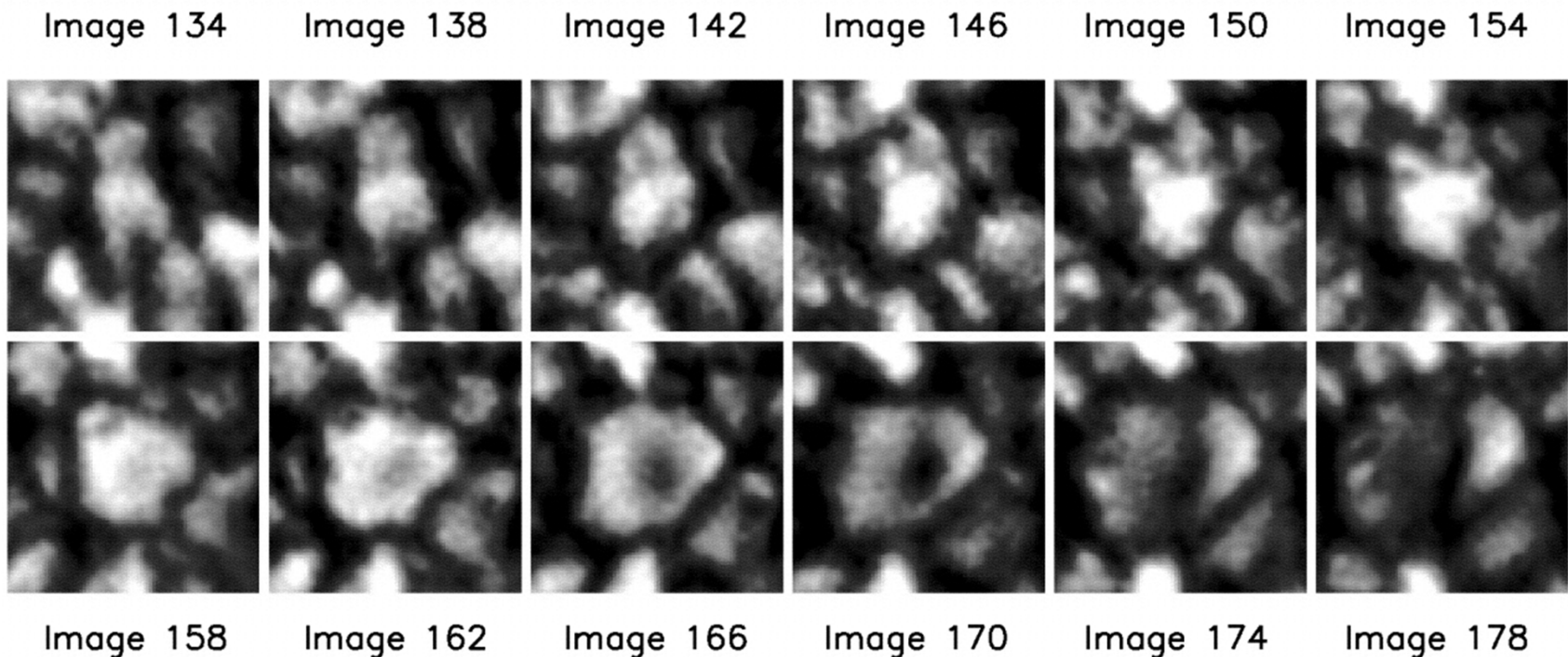
The convective overshoot of the gas flow from the solar convection zone into the photosphere forms a pattern of bright cellular elements the granules, surrounded by a network of dark intergranular lanes



Movie of solar granulation observed with adaptive optics



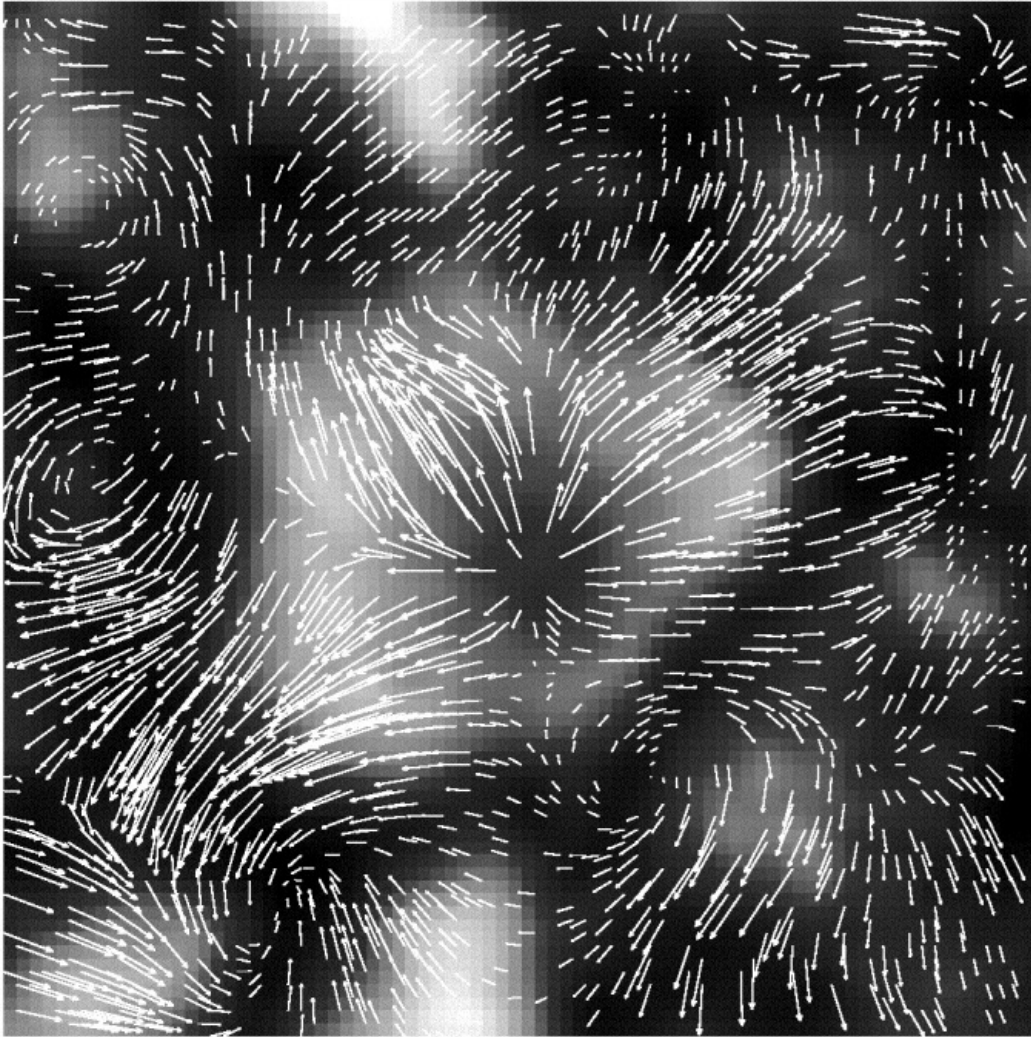
"Exploding granules" have become a well-known solar surface phenomenon. They are described as bright and rapidly expanding granular cells containing a dark spot in their centers, forming a ringlike structure that fragments into several smaller granules



Twelve snapshots of the life of a typical undisturbed exploding granule.

The time range is about 13.5 minutes, and the size of the panels is approximately 5×5 arcsec.

Flow field in exploding granules



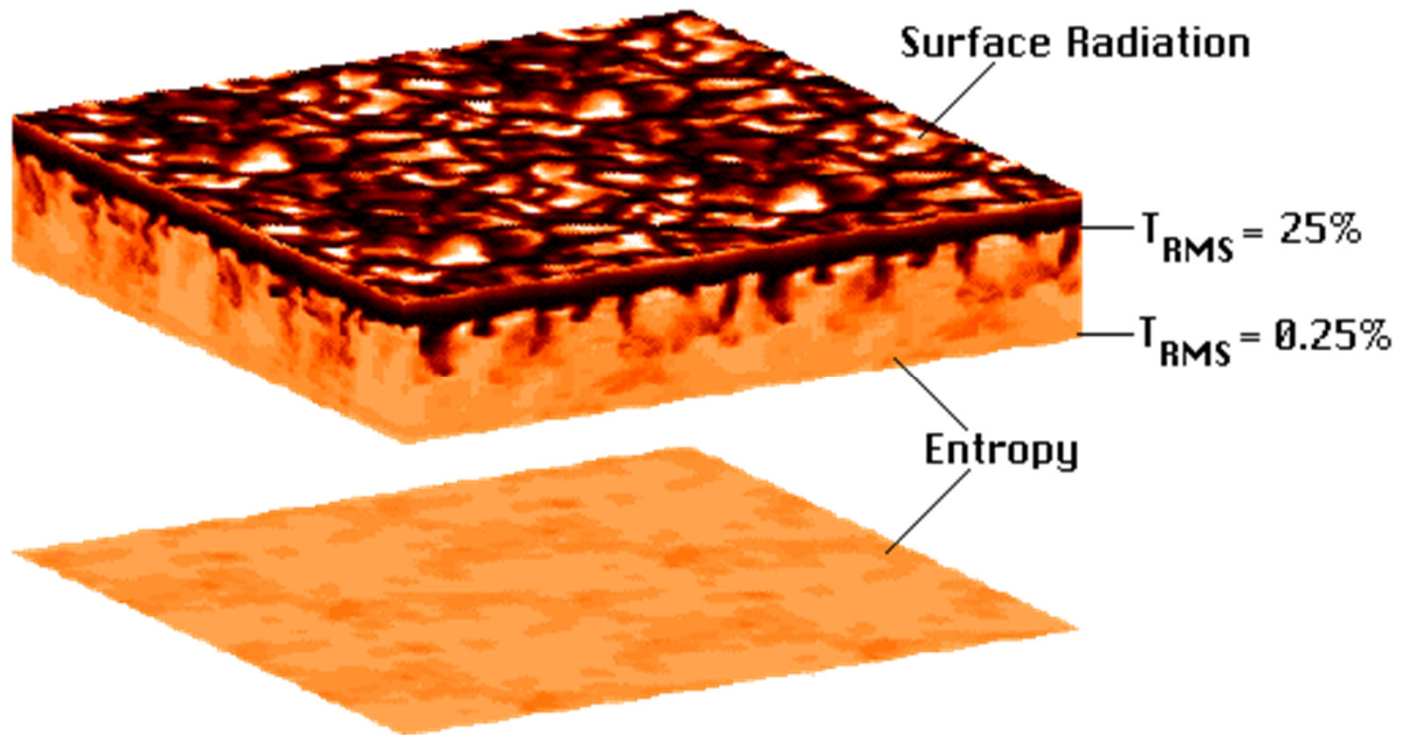
Flow field of the exploding granule. The maximum velocity is 4.38 km/s, and the mean velocity is 1.17 km/s.

The evolution of exploding granules and dark dots seems to be strongly driven by the formation of downflows.

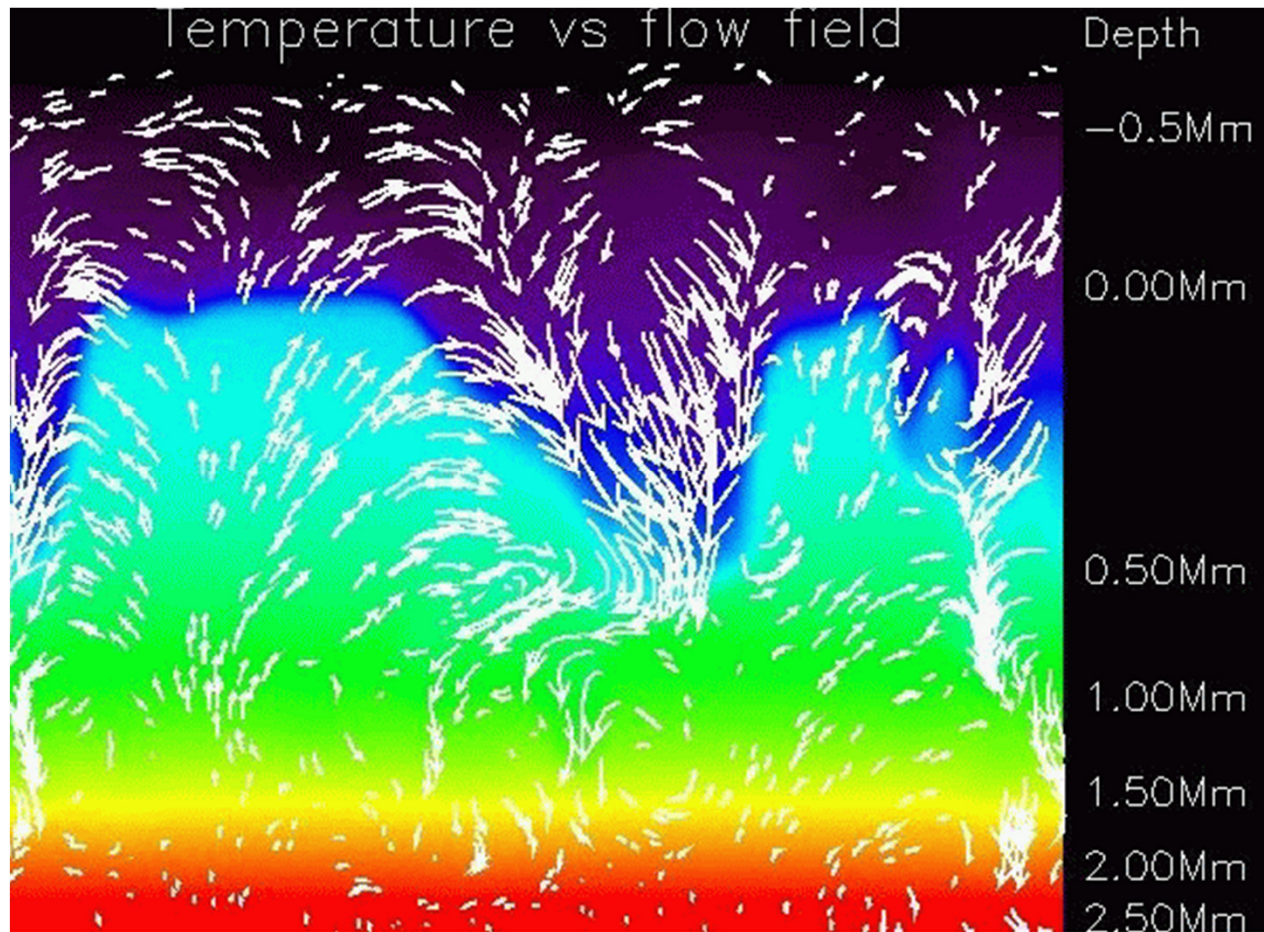
This picture of the evolution of exploding granules agrees well with model simulations that granulation is mainly driven by spontaneously developing downflows due to thermal instabilities in the convective flows.

Some of these downflows could also have high angular velocities leading to a high stability similarly to tornados in the Earth's atmosphere, which are more stable the faster they rotate.

This interpretation of some central downflows as rotating "bathwater" may be an explanation of the relative stability and dynamics of the dark dots found in our data material.

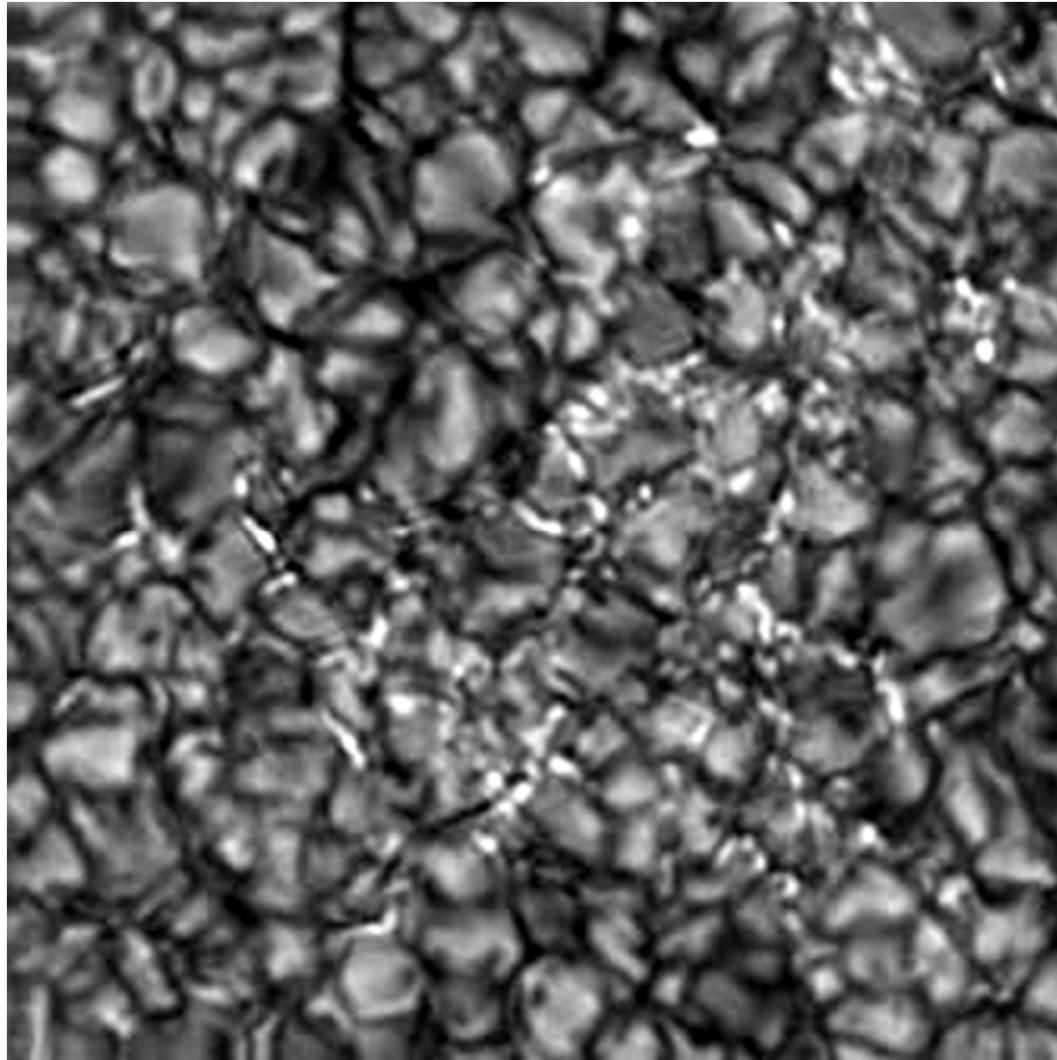


Numerical simulation of granulation.

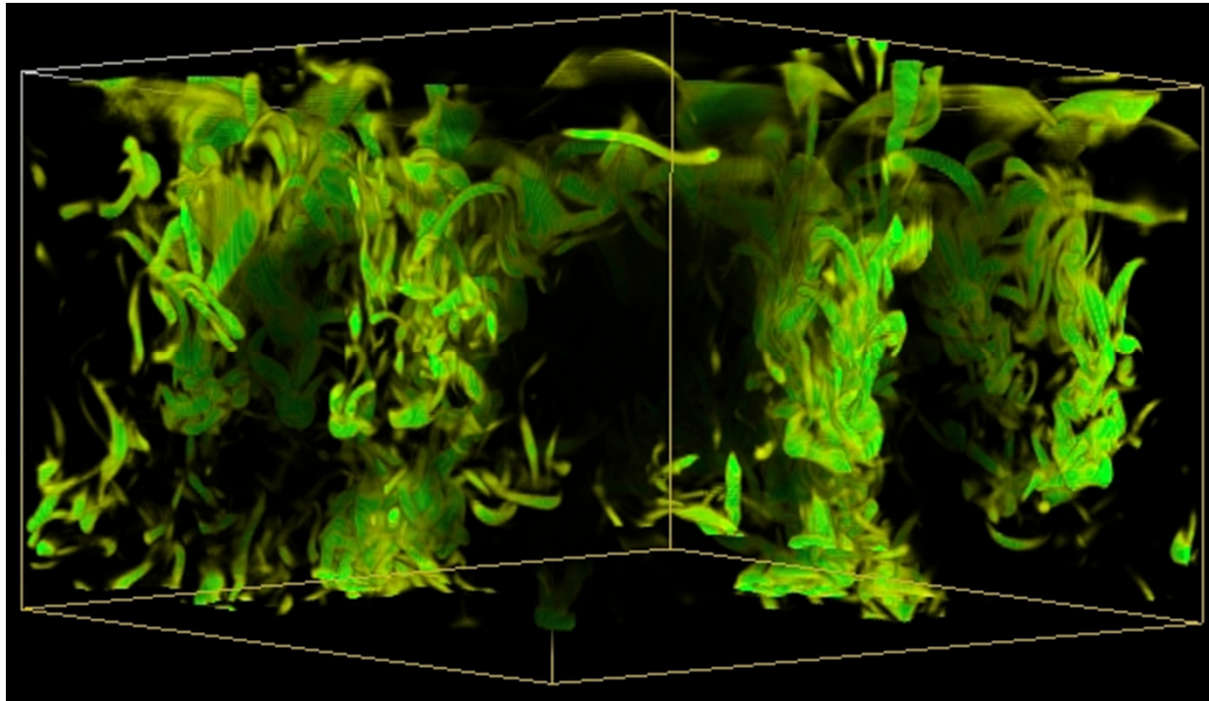


Numerical simulation of downflows in granules.

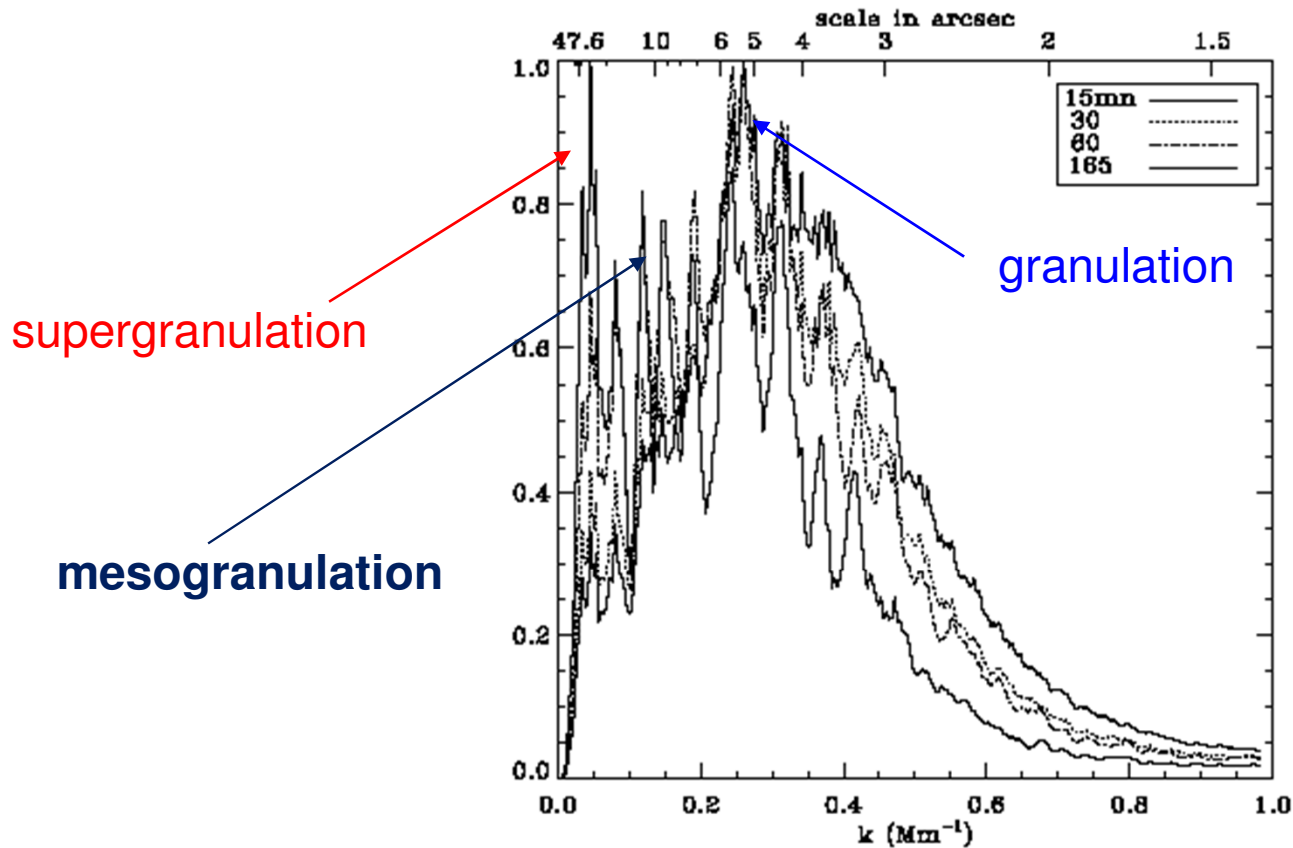
Concentrations of magnetic flux tubes ($B \sim 1$ kG) in the intergranular lanes



Numerical simulations reveal flow vorticity in the convection downdrafts in the intergranular lanes



Spectral properties of solar convection



1 arcsec = 720 km

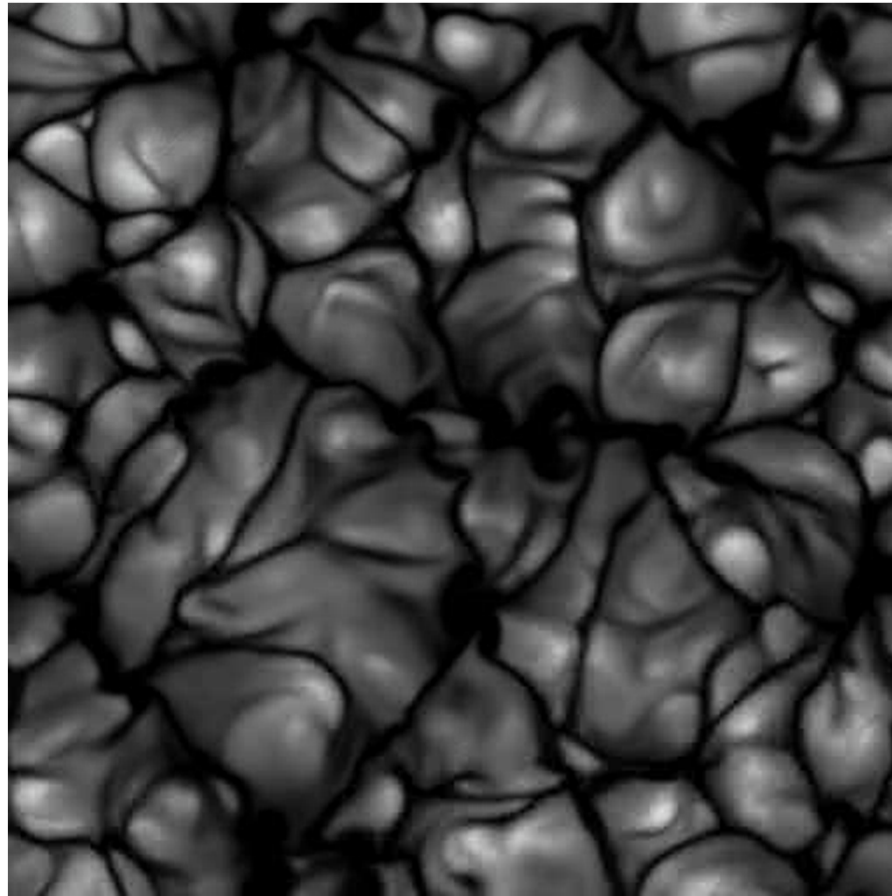
Granulation size ~
3,000-4,000 km

Mesogranulation size ~
7,000-8,000 km

Supergranulation size
~ 30,000-40,000 km

Fig. 1. Power spectra $E_\tau(k)$ of the horizontal velocity fields using the three hour data set of Pic du Midi. The grid size is $0''7$ ($1'' = 728$ km); note that the field of view is $58.2'' \times 47.6''$. All the spectra have been normalized by their maximum value. The different line styles refer to the time-averaging window of size τ .

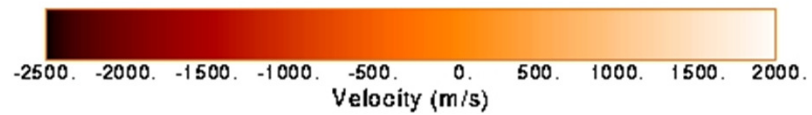
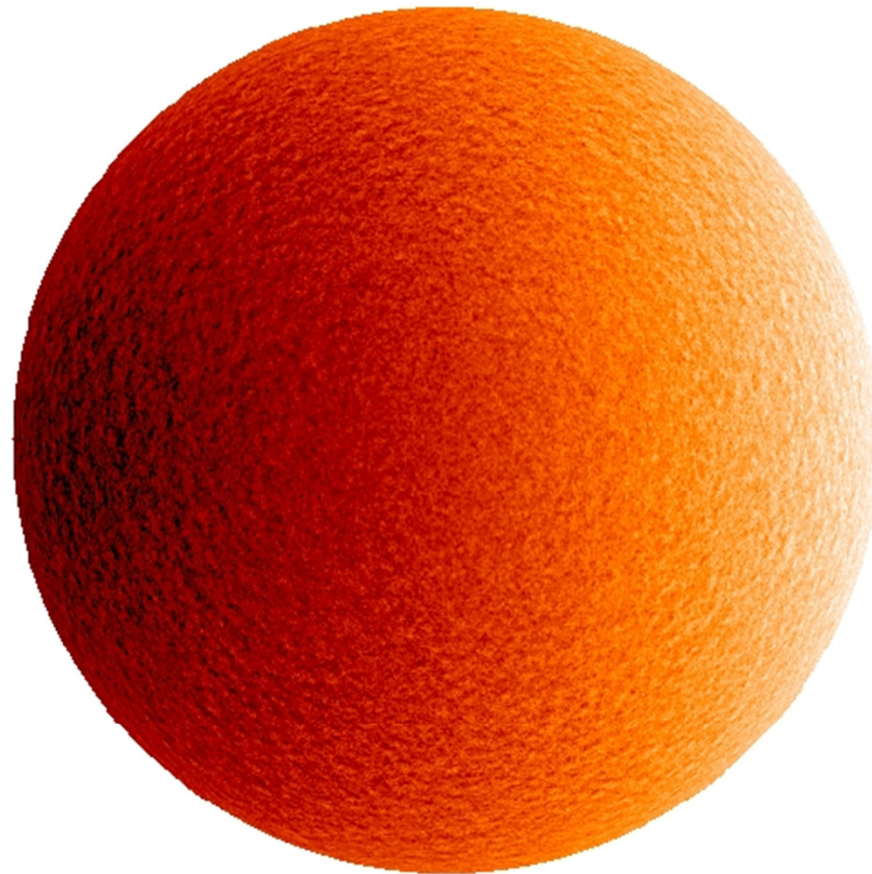
Mesogranulation – clustering of granules – no clear observational picture



Numerical simulation by Cattaneo et al

Single Dopplergram

(30-MAR-96 19:54:00)



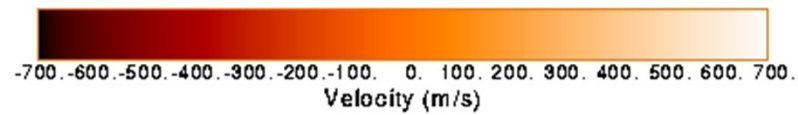
SOI / MDI

Stanford Lockheed Institute for Space Research

The rotation speed of the solar surface is 2km/s.

Average Dopplergram Minus Polynomial Fit

45 images averaged (30-Mar-96 19:26 to 30-Mar-96 20:17)

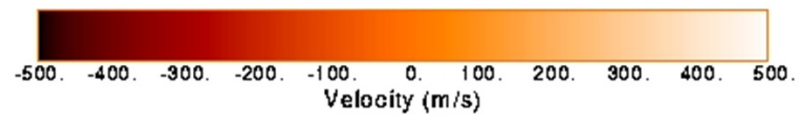


SOI / MDI

Stanford Lockheed Institute for Space Research

Single Dopplergram Minus 45 Images Average

(30-MAR-96 19:54:00)



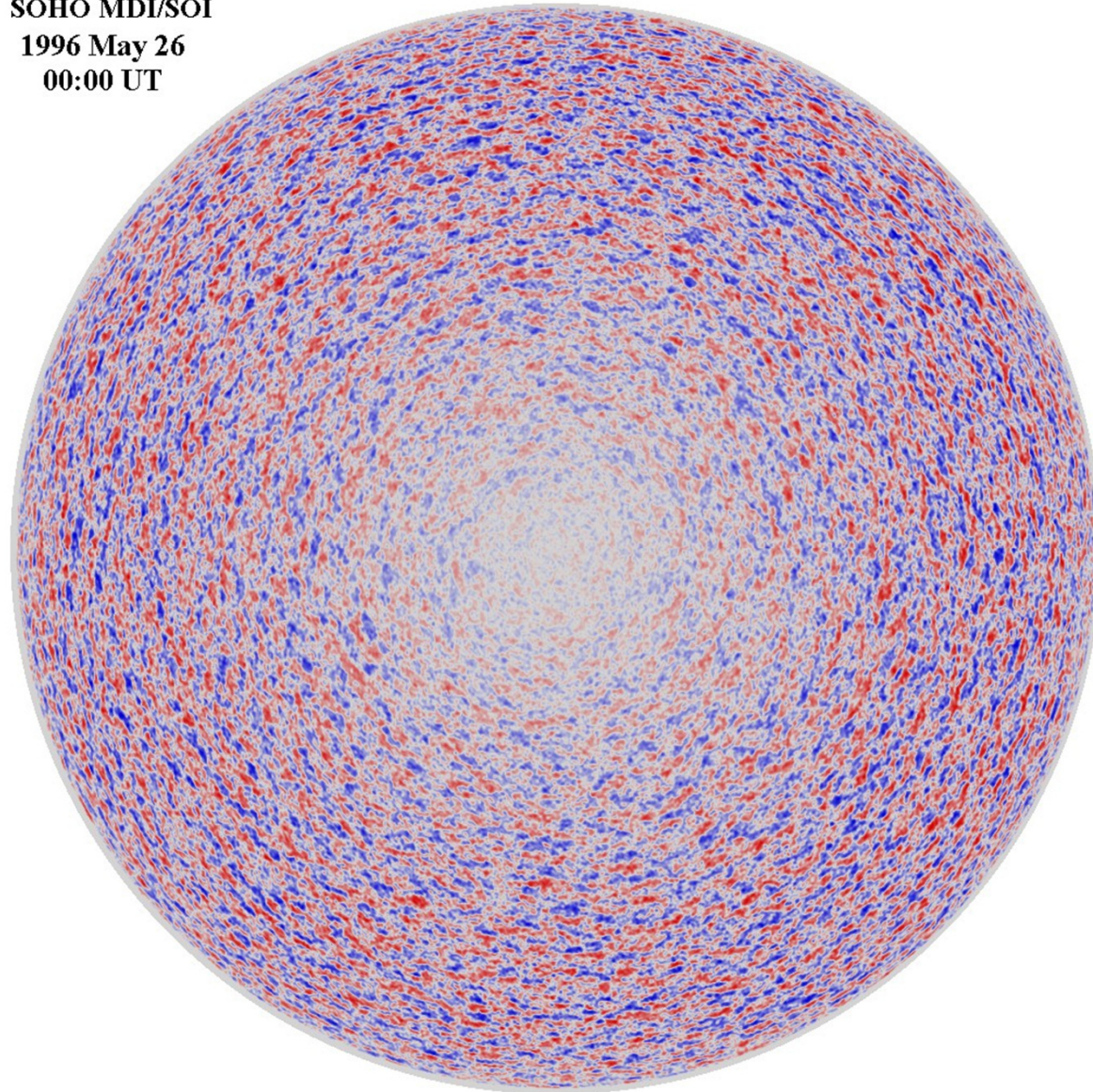
SOI / MDI

Stanford Lockheed Institute for Space Research

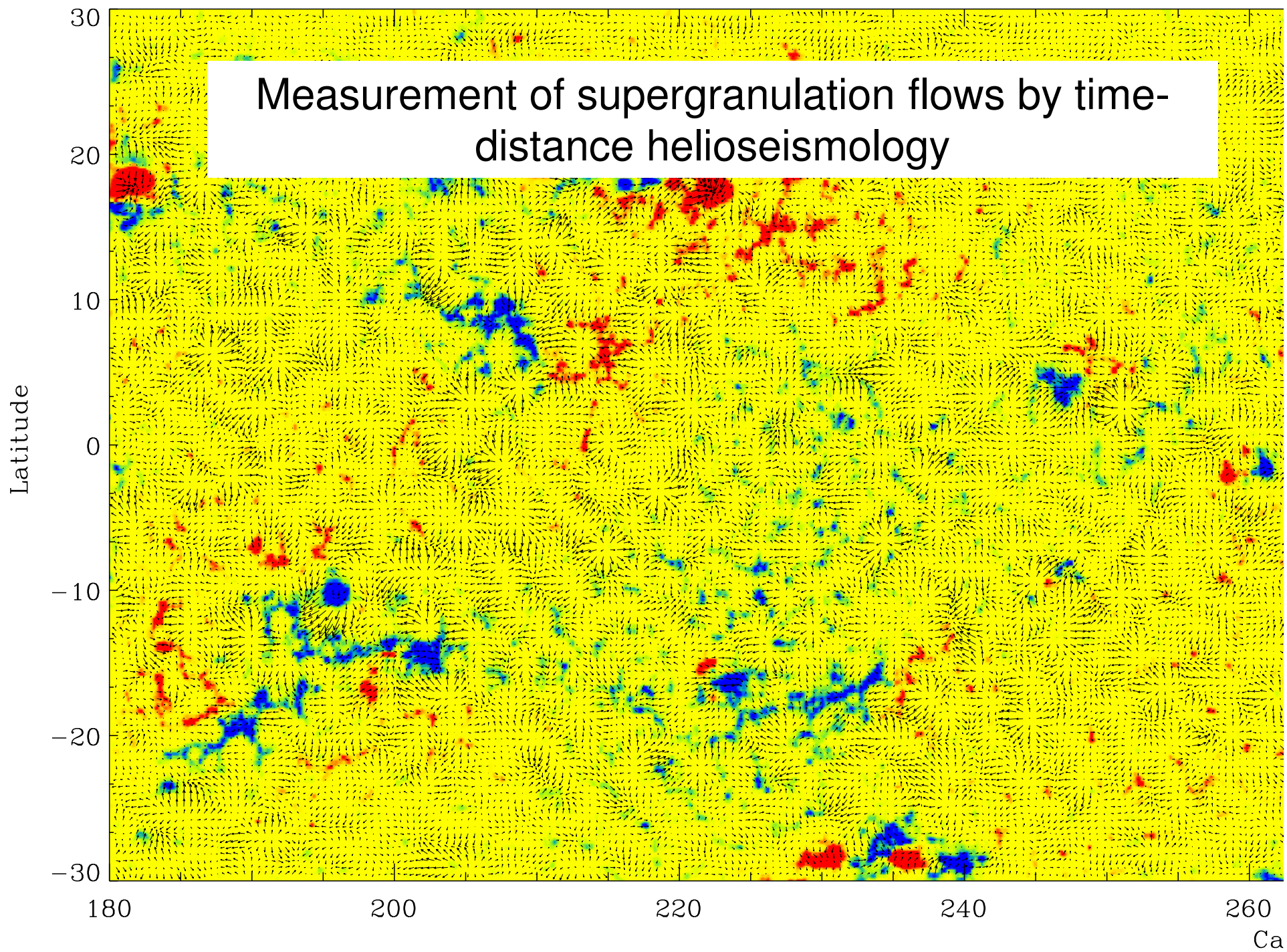
Supergranulation

Doppler shift
observations

SOHO MDI/SOI
1996 May 26
00:00 UT



Measurement of supergranulation flows by time-distance helioseismology



Origin of supergranulation

Origin of supergranulation – increased convective instability in the He II ionization zone (second ionization of helium), located 15 Mm below the photosphere (Simon & Leighton, 1963), due to the decreasing adiabatic exponent $\gamma < 5/3$.

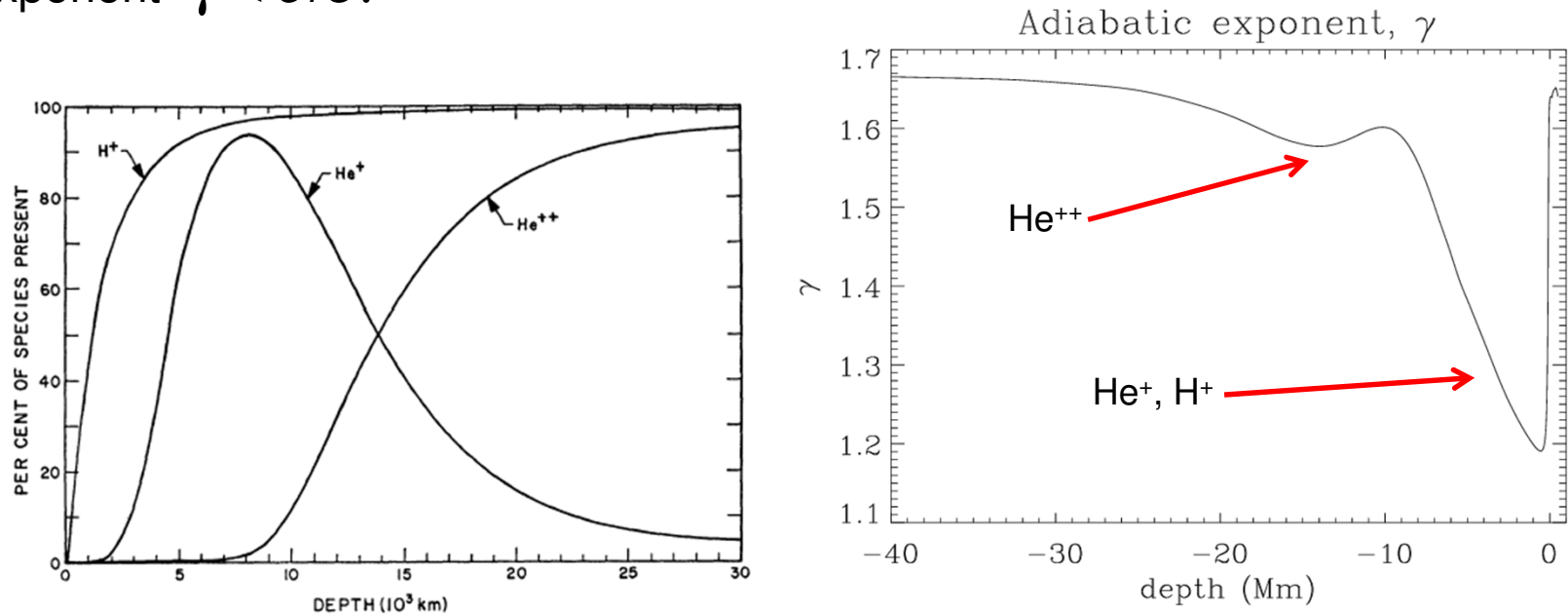


FIG. 12 — Ionization of hydrogen and helium in the convective envelope of the Sun. Depth is measured relative to optical depth $2/3$ in the continuum. Unpublished data of Iben and Sears (1962).

For an ideal gas $\nabla_{ad} \approx \frac{\gamma-1}{\gamma}$, thus the instability occurs when $\nabla > \frac{\gamma-1}{\gamma}$.

In fully ionized gas $\gamma = 5/3$; thus, $\nabla = (\gamma-1)/\gamma = 0.4$ in the ionization zones $\gamma < 5/3$, such zones are more unstable.

Search for giant cells

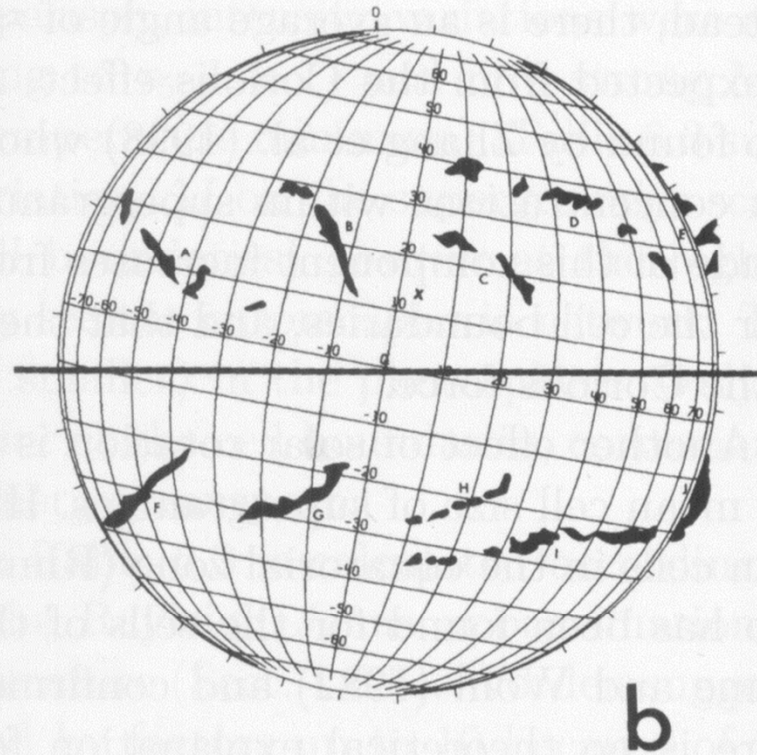
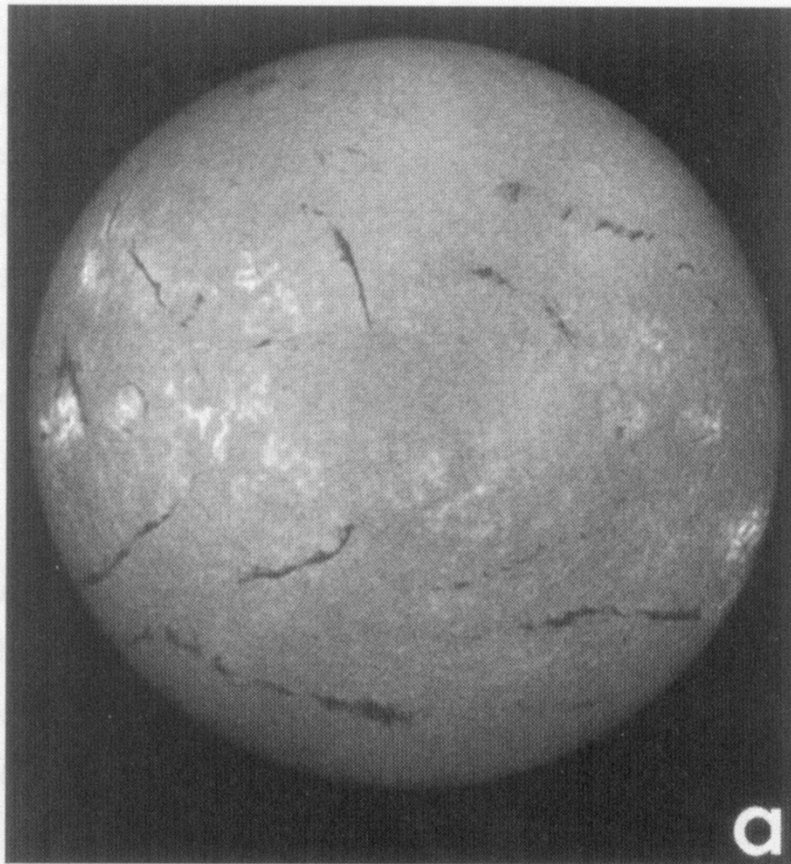


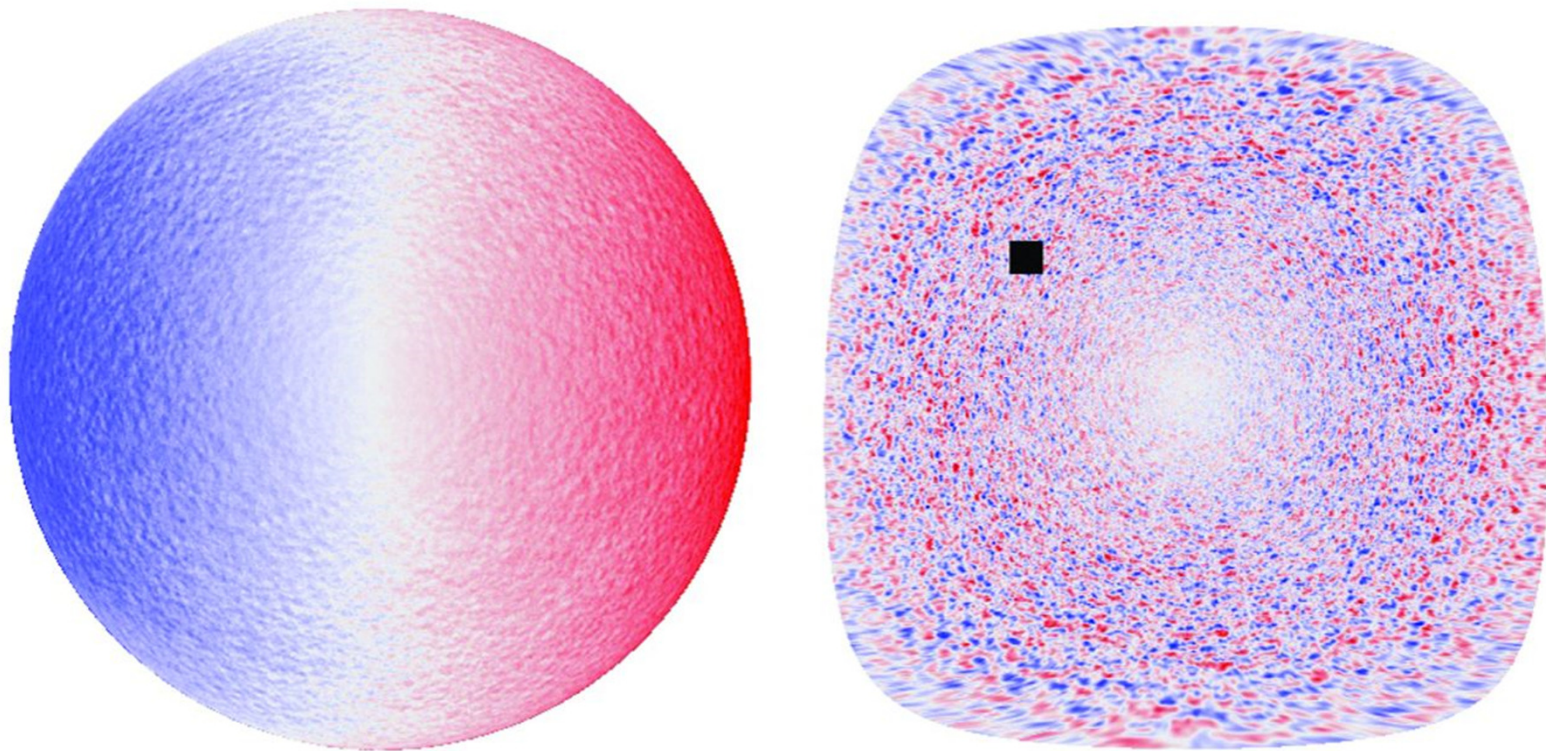
Fig. 6.22. Distribution of solar filaments on 11 June 1972 (Wagner and Gilliam 1976). Courtesy National Solar Observatory, AURA, Inc.

Science 6 December 2013:

Vol. 342 no. 6163 pp. 1217-1219

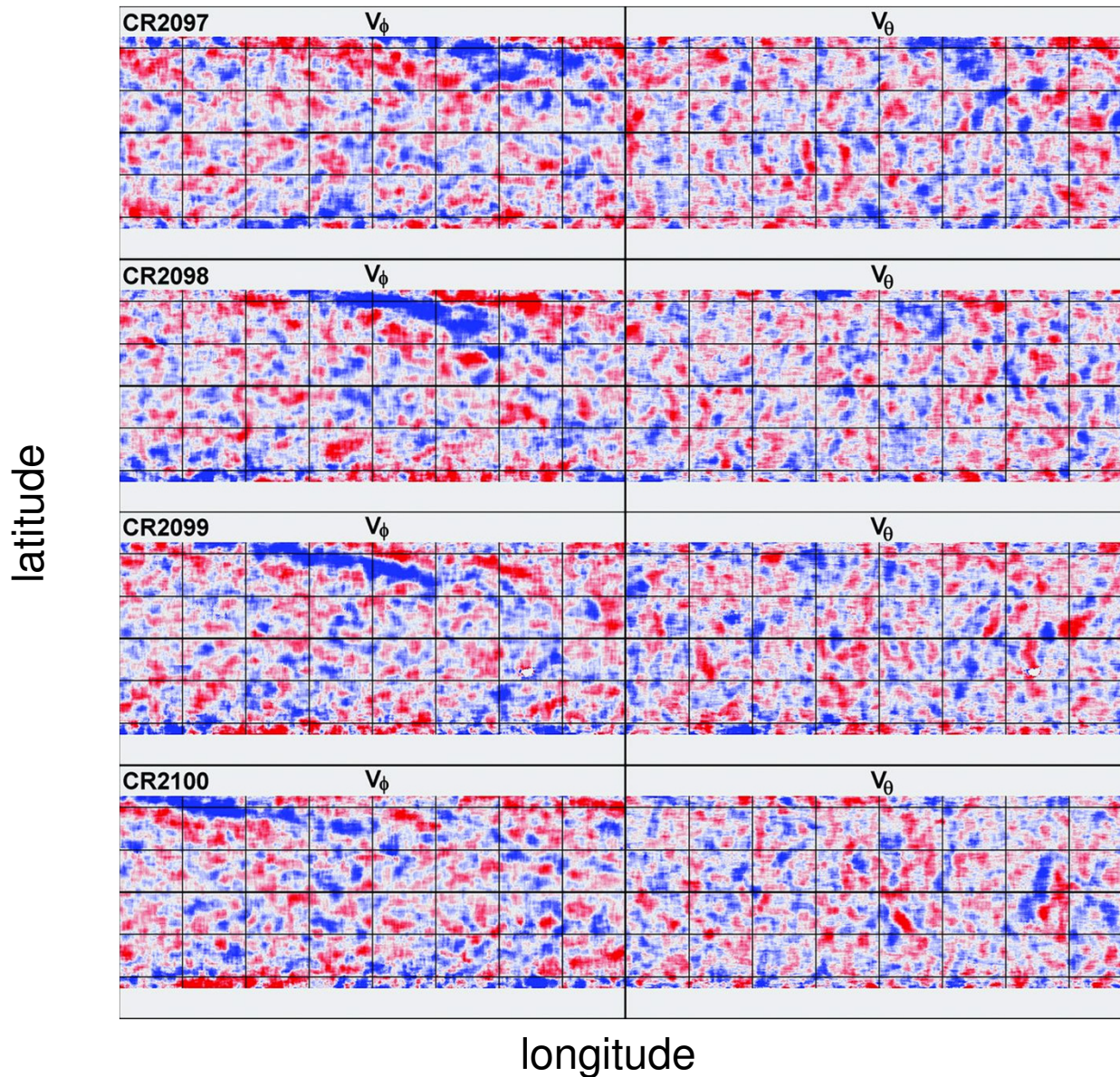
Giant Convection Cells Found on the Sun

David H. Hathaway, Lisa Upton, Owen Colegrove



They found evidence for giant cellular flows that persist for months by tracking the motions of supergranules.

Evidence for Giant Convection Cells



A sequence of supergranule flow velocity maps shows persistent large-scale patterns.

Numerical simulations of convection in a rotating sphere have not explained the multi-scale structure of solar convection but reproduced the differential rotation

